Rates of CH_4 Displacement by a N_2-CO_2 Mixture in CH_4 Hydrates

Elizabeth Coward, Monterey Bay Aquarium Research Institute
Mentors: Peter G. Brewer, Edward T. Peltzer, and Peter M. Walz
Summer 2011

Keywords: laser Raman spectroscopy, methane hydrate, CH_4 displacement, in-situ analysis

Abstract

Methane hydrates have been investigated for their potential as both a source of natural gas and a carbon dioxide sink. Many studies have successfully created CO_2 hydrate from a methane hydrate substrate in a laboratory setting. Yet these analyses rely on induced exchange generated within closed pressure cells - allowing for the formation of hydrates under conditions that do not accurately represent natural geologic systems. The proposed mechanism for this reaction, a simple one-for-one substitution driven by a N_2-CO_2 displacement gas mixture for the displacement of CH_4 by CO_2, is thermodynamically possible but remains mechanistically unproven; and the validity and extent of such an exchange occurring under natural conditions was previously untested. In March of 2010, a Brewer lab/USGS team exposed a synthetic CH_4 hydrate to a N_2-CO_2 gas environment within a glass chamber on the sea floor of Monterey Bay, CA. This multi-phase system failed to produce a CO_2 hydrate, but instead resulted in the sublimation of the original CH_4 hydrate and development of a water and ternary gas mixture. This reaction was monitored both visually and with DORISS2, the Deep Ocean Raman In-Situ Spectrometer producing spectra of both the gas space and the solid hydrate over the course of 24 hours. Pressure profiles of binary and ternary gas standards were used to calculate the calibration values necessary for analysis of the in-situ spectra. These calculations, in addition to physical observations, suggest that the previously suggested substitution reaction forced in a pressure vessel does not occur under the more open static in-situ pressure and temperature conditions examined here. This suggests the unlikelihood of this reaction occurring on a large scale within geologic formations containing methane hydrates.

Introduction

Displacement of CH_4 by CO_2 in methane hydrates has been proposed as a mechanism for sequestering CO_2 and simultaneously accessing the carbon reserve stored within the large hydrate deposits occurring along continental margins and permafrost areas. The injection of CO_2 into CH_4 hydrate has been completed successfully in CO_2-rich high-pressure cells with synthetic and recovered hydrate samples [Ota et al., 2005; Stevens et al., 2008; Svandal et al., 2006; Zhou et al., 2008]. Park et al [2006] have proposed a mechanism for this reaction, suggesting that it is a simple one-for-one substitution driven by a N_2-CO_2 displacement gas mixture in which the primary cage structure shifts and CH_4 is released to allow for the formation of CO_2 hydrate, which is thermodynamically favored [Lee, 2003]. How this exchange would occur on both a molecular and a macroscopic level, however, has not yet been elucidated. Equally unclear is how such a process would occur on a large scale in-situ with lower pressures and in an unstirred saline, aqueous geologic environment quite different from the suite of pressure vessel studies that have been undertaken [Husebø et al., 2008; Graue et al., 2006; Stevens et al., 2008]. A field experiment to test this process on a scale large enough for fluid flow within the apparatus to occur was undertaken by the Brewer lab/USGS team in 2010. This paper details the first analysis of the results of this experiment.

Background

In March 2010, the Brewer lab team together with USGS colleagues conducted an experiment in which a synthetic, pure CH_4 hydrate stick was brought to the sea floor in Monterey Bay within a pressure vessel using ROV Ventana, removed from the pressure vessel, and placed inside a Pyrex container filled with a N_2-CO_2 gas mixture (75.0% N_2, 25.0% CO_2). The gas mixture was chosen to simulate that of the Park et al. [2006] experiment. The system within the container was then monitored optically and spectroscopically. A visual overview of the experiment is included below.

The technique used to monitor the course of the experiment was in situ Raman spectroscopy, achieved by focusing the laser through the walls of the container and examining the changing composition of both the gas and solid phases through time during the course of the experiment *[See Appendix]*. The experiment was made possible by innovations in application of laser Raman spectroscopy to in situ deep ocean geochemistry [Brewer et al., 2004; Zhang et al., 2010]. Initial use of Raman techniques for the study of hydrate structure and composition in the laboratory was established by Sum et al [1997], and the development of a deep-ocean laser Raman spectroscopy system by Brewer et al. [2004] proved critical for the in-situ identification of an ever-changing hydrate profile and gas composition in this experiment.

Methods

Laser Raman Spectroscopy. Analysis of the in-situ spectra gathered from Monterey Bay in March 2010 required complementary Raman laser spectroscopy in a controlled setting, both for calibration of the laser system itself and for generating thermodynamic profiles of known, quantifiable standards. For this work, a bench-top laser Raman system was employed. Gas cylinders were sourced to a pressure cell containing a sapphire window, the pressure of which was manually controlled. The temperature of the cell was decreased and maintained with a chilled water circulation system.

Gas Standard Fabrication and Processing. Four CH_4/N_2 mixtures of 0.10, 0.20, 0.30 and 0.40 mol ratios, and four CO_2/N_2 mixtures of 0.05, 0.10, 0.15, 0.20 mol ratios, were generated in 1500 psi stainless steel cylinders. Gas standard cylinders were filled to known composition by weight. Cylinders were evacuated and subsequently filled with their identifying gas and nitrogen, with final pressure summing to 1785 psi. Cylinders were weighed after each component gas fill to ensure accurate ratios. Each cylinder was connected to the pressure cell, maintained at a constant temperature of 4.0° C, and subsequently released, pressurizing the cell to the full potential. Pressure was then released incrementally by 100 psi units and a Raman spectrum was taken with each decrease.

Spectrum Integration. Spectra observed were produced by HoloGRAMs software, and processed with GRAMS AI. All spectra were corrected for baseline inaccuracies. Peaks were located, fit and integrated using a high sensitivity scan looking for both Lorentzian and Gaussian distributions. The integrated values were then exported from GRAMS AI into Excel and Matlab for further analysis.

CO_2 Dyad Analysis. Initial analysis of a 2:1 N_2: CO_2 gas mixture generated in the laboratory highlighted a known physical phenomenon manifest in the data. The Raman signal of CO_2 is a Fermi dyad, two small peaks of similar dimensions arising from accidental degeneracy. In producing a pressure profile with 100 psi increments, it appears that each of the dyad peaks responds differently to increasing pressure, producing complementary CO_2/N_2 ratio curves. In order to reconcile the disparate Raman cross-sections, the sum of the two dyad peak areas was used in compositional and rate calculations. In contrast, both CH_4 and N_2 gases produce a dominant peak.

Rate calculations. From these eight pressure profiles, relative molar response factors (mRF) were calculated for later use in analysis of the March 2010 spectra. For each gas cylinder, the actual concentration ratio was calculated, and lines were fit to the data using the method of least squares where the mRF is a function of pressure:

$$\text{mRF} = \text{slope} * P_{abs} + \text{intercept} \qquad \textit{Eq. 1}$$

The experimentally observed peak area ratios were divided by mRF values to calculate the observed gas composition within the hydrate pressure vessel:

$$CO_{2\,\%} = 100\ [CO\text{-Peak Area}/N_2\text{-Peak Area}]/mRF \qquad \textit{Eq. 2}$$

$$CH_{4\,\%} = 100\ [CH_4\text{-Peak Area}/N_2\text{-Peak Area}]/R \qquad \textit{Eq. 3}$$

CO_2/N_2 Mixtures –

Pressure dependent mRF equation coefficients

Cyl #	Mole Ratio	Slope	Std dev.	Intercept	Std dev.	R	mRF at P1	mRF at P2
1	0.0593	0.0051	0.0013	1.1664	0.0721	0.8839	1.699	1.525
2	0.1172	0.0002	0.0006	1.3716	0.0355	0.1270	1.392	1.385
3	0.2130	0.0026	0.0013	1.2323	0.0744	0.6167	1.507	1.417
4	0.3240	0.0013	0.0011	1.3260	0.0632	0.4079	1.459	1.415
						Mean	1.514	1.436
						Std dev.	0.132	0.061

CH_4/N_2 Mixtures –

Pressure dependent mRF equation coefficients

Cyl #	Mole Ratio	Slope	Std dev.	Intercept	Std dev.	R	mRF at P1	mRF at P2
5	0.1087	0.0047	0.0007	9.4301	0.0391	0.9372	9.923	9.762
6	0.2928	0.0139	0.0022	8.5342	0.1387	0.9124	9.991	9.514
7	0.4904	0.0125	0.0016	8.6081	0.098	0.9432	9.915	9.488
8	0.7557	0.0148	0.0016	8.2510	0.1045	0.9528	9.800	9.294
						Mean	9.907	9.514
						Std dev.	0.079	0.192

Ternary Gas Standards. Additionally, ternary gas standards were generated mimicking the final composition of the gas space spectra. Pressure profiles were created using the same methodology. These ternary standards were compared against the binary standards in order to determine if any additional inter-molecular interactions were occurring within the ternary mixture as the pressure varied. Peak ratios at set pressure and temperature were compared against those calculated from the binary standards at equal conditions. The mRFs differed minimally, with an average variance of 3.0%.

Results

All spectra accumulated during the March 2010 Point Lobos dives and generated from standards developed in the Brewer laboratory were processed with GRAMS AI spectroscopy software, allowing for baseline corrections and peak integration. Peak dimensional values were then exported to Excel and Matlab for further manipulation. Area ratios were calculated and subsequently corrected for Raman cross-section pressure sensitivity. As detailed in Methods, the peak area ratios were used to calculate gas composition. In the construction of standard pressure profiles, these compositions were calculated with decreasing pressure and at a set temperature to determine the effect pressure has on the Raman cross-section intensity. There is a linear relationship between the cell pressure and the intensity of the Raman signal, regardless of gas identity, indicating that all standards used in the analysis of the in-situ spectra required similar temperature and pressure conditions.

Binary and ternary gas standards were created in the Brewer laboratory by weight. Spectra were gathered at 100 psi decreasing increments from the initial cylinder pressure. Matlab was used to calculate least squares fit lines, slope, intercept and component standard deviations *[Table 1]*, mRF values were calculated for each of the cylinders. The mean of these were then used to calculate the composition of the in-situ gas space *[Eq.2 & Eq.3]*.

As shown in Figure 2.1, a distinct increase in CH_4 composition occurs immediately within the gas space, indicated by the sharp slope of the red data points. The first Raman spectra, which occurred mere seconds after the cylinder placement, suggests a composition of 75.2% N_2 : 24.2% CO_2 : 0.6% CH_4, indicating the rapidity with which the reaction occurs. N_2 and CO_2 concentrations, contrastingly, decrease quickly and maintain a negative trend throughout the course of the dive. Thus it is clear that the methane hydrate is dissociating rapidly within this high-CO_2 environment and that N_2 and CO_2 gas are both being removed from and diluted within the gas phase.

However, the sublimation of the CH_4 gas and melting water creates a complex, mixed-phase system in which the pressure within the cylinder is constantly increasing at inconsistent rates. The CO_2 gas is dissolving into the water as the heterogeneous gas itself is potentially forced under the base of the cylinder in this constant pressure experiment, effectively leaving the system.

The rate of change of CH_4 concentration in the gas phase decreases markedly over the course of the day. We report this as a polynomial fit to the data, suggesting an approaching plateau. The CH_4 data from Figure 2.1 have been grouped into three distinct sampling sections, as seen in Figure 2.2, and the linear fit of each set plotted separately.

We observed a significant decline in the rate of reaction from the first sample set to the final set, almost halving over 0.1 day fraction. The change in percent composition leveled by the second day *[Figure 3]*, ending at a final distribution of 70.6% N_2 : 21.6% CO_2 : 7.8% CH_4. As such, gas space N_2 and CO_2 concentrations decline between the two dive days, but remain dominant. This change in composition is summarized by Figure 4.

Discussion and Conclusions

The March 2010 experiment, designed to test the potential for in-situ generation of CO_2 hydrate from a CH_4 hydrate substrate, highlighted the shortcomings of the current displacement hypotheses. With the hydrate gas : solid ratios used here we found no evidence of formation of a solid CO_2 hydrate despite the initial saturated-CO_2 environment. It appears that the proposed binary substitution is not achieved under the conditions used here.

It also appears that it would be very difficult to achieve this substitution within a geologic formation, and on a much larger scale. The exact mechanism of CH_4:CO_2 exchange proposed by Park et al. is mechanistically unstated but is described as a “swapping”. Since discussion of the transition to a liquid-water state followed by re-formation of a CO_2 hydrate is carefully avoided, the impression is of potential partial opening of the hydrate cage, exiting of the CH_4 guest and occupation of the space by CO_2. We failed to observe this, yet we did observe the steady disappearance of the CH_4 hydrate phase and the creation of a thin film of liquid water. This flowed to the bottom of the apparatus becoming enriched in dissolved CO_2, and was expelled slowly from the base of the gas cylinder by rising gas pressure.

It is difficult to conceive of rapid exchange in a system in which the hypothetical accumulation of a rind of solid CO_2 hydrate on the surface must form an effective barrier to further diffusion of CH_4 gas. As such, the formation of CO_2 hydrate would be limited to a relatively thin layer. In addition the very high solubility of CO_2 in water - some 10x that of CH_4 - must result in large losses of CO_2 from the gas phase into the produced liquid and make maintaining any proposed optimal gas mixture concentration very difficult.

These data, in congruence with the physical observations of the lack of hydrate development, suggest that the complex, mixed-gas-liquid-solid phase system that develops in-situ does not replicate the mechanisms seen in laboratory pressure cells. Our standards proved accurate, allowing comprehensive integration of the March 2010 spectra and an understanding of the thermodynamics of a hydrate-gas interface.
From the rate calculations detailed within this report, a phase diagram can be constructed outlining the boundary for formation of a pure CO_2 hydrate at two similar sites in Monterey Bay, Hydrate Hill and Hydrate Hotel *[Figure 5]*. The work of Park et al yields a 5.0 - 10.0% CH_4 residue, despite the high pressure and low temperature, only 10.0 - 15.0% lower in CH_4 than that of the Brewer Team. Thus it is appears difficult to produce a pure CO_2 hydrate by this process within the laboratory, and likely not possible under realistic in-situ conditions where a mobile aqueous phase must be present.

Appendix

Raman spectra are derived from the inelastic scattering of a monochromatic light source, causing an observable change in the vibrational state of the target molecule. This Raman shift results when the change in energy from the initial vibrational state is positive in sign ($v_0 - v_m$), where v_m is the vibrational frequency and v_0 is the incident beam. Anti-stokes shift ($v_0 + v_m$) is the complementary decline in energy. Raman shift is calculated as follows:

$$P = \alpha_0 E_0 cos2\pi v_0 t + (\partial\alpha / \partial q)_0 + q_0 E_0 cos2\pi v_0 t cos2\pi v_m t$$ [Ferraro et al., 2003]

Where P is the electric dipole moment induced, α_0 is the polarizability at the equilibrium position, E_0 is the vibrational amplitude of the electric field strength, $(\partial\alpha / \partial q)_0$ is the rate of change of α with respect to the change in q at the equilibrium position, and q_0 is the vibrational amplitude of the nuclear displacement [Ferraro et al., 2003].

Figures

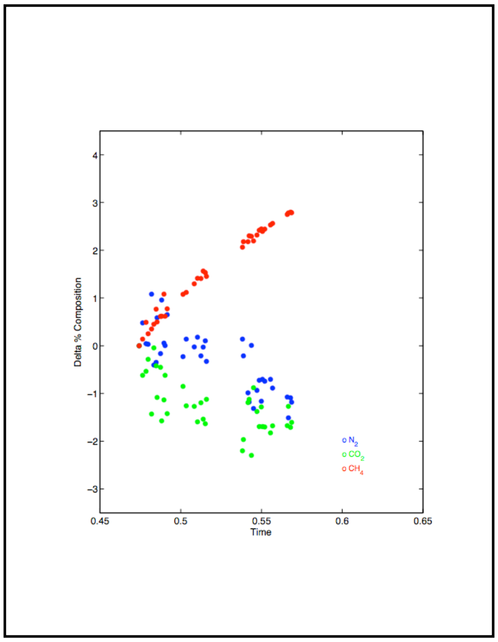

Figure 2.1. Change in gas space percent composition, dive day 1.

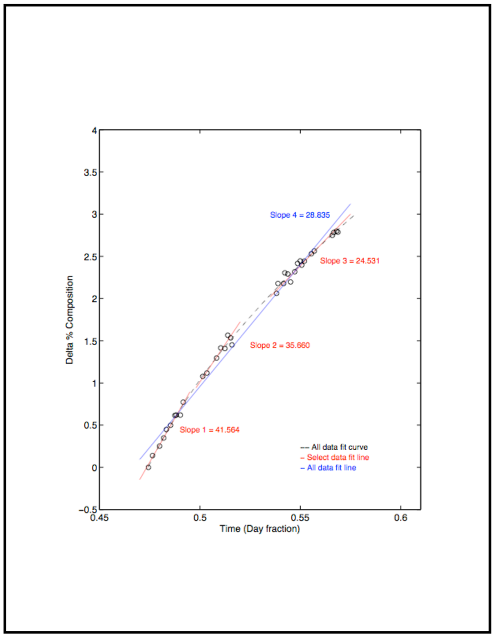

Figure 2.2. Close examination of CH_4 data.

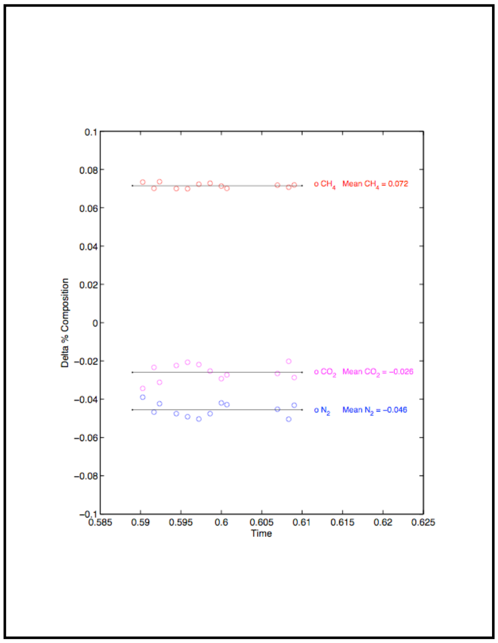

Figure 3. Change in gas space percent composition, dive day 2.

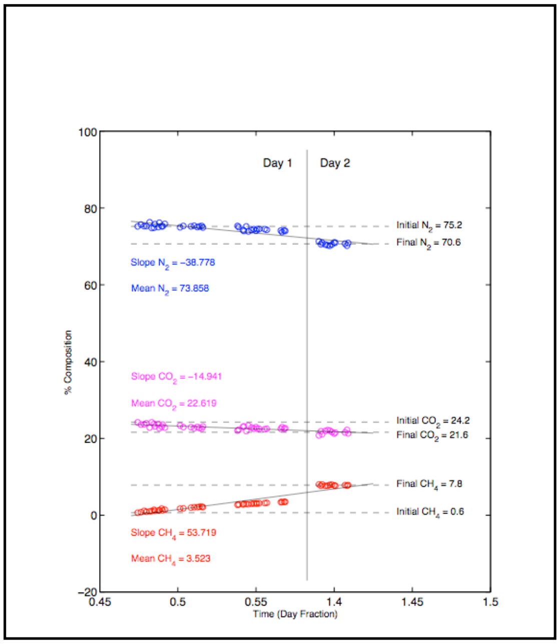

Figure 4. Evolution of the gas space percent composition, dive day 1 - 2.

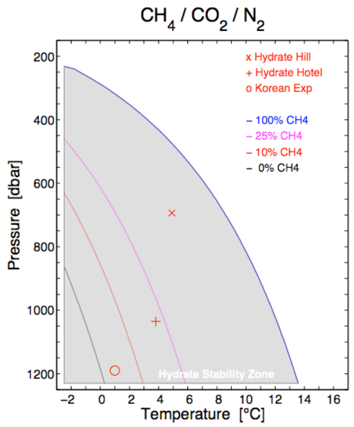

Figure 5. Phase diagram of hydrate stability in a $CH_4/CO_2/N_2$ mixed gas environment.

Acknowledgements

I acknowledge the David and Lucile Packard Foundation for the funding of this intern research project. Principal thanks to mentors Peter Brewer, Ed Peltzer and Peter Walz for their invaluable help and support over the ten weeks. The Brewer team continues to be an endless source of knowledge, experience and intellectual curiosity, for which I am incredibly grateful. Thank you also to George Matsumoto and Linda Kuhnz for their dedication to the MBARI internship program and the individual success of each intern. A special thank you is extended to the crew of the *R/V Western Flyer* and pilots of the ROV *Doc Ricketts* for their enthusiasm and commitment to ocean exploration.

References

[1] P. Brewer, G. Malby, J. Pasteris, S. White, E. Peltzer, B. Wopenka, J. Freeman and M. Brown, Development of a laser Raman spectrometer for deep-ocean science, *Deep-Sea Res.* **51** (2004), pp. 739–753.

[2] Ferraro, J., Nakamoto, K., Brown, C., 2003. Introductory Raman Spectroscopy, 2nd ed. Academic Press, San Diego.

[3] Graue A, Kvamme B, Baldwin B, Steven JC, Howard JJ, Ersland G, Husebø J. *Magnetic Resonance Imaging of Methane- Carbon Dioxide Hydrate Reactions in Sandstone Pores.* In: SPE Ann Tech Conf, 24- 27 Sept, 102915-MS, San Antonio, 2006.

[4] Husebø J, Stevens JC, Graue A, Kvamme B, Baldwin BA, Howard JJ. *Experimental investigation of methane release from hydrate formation in sandstone through both hydrate dissociation and* CO_2 *sequestration.* In: Proc. Intl. Conf. Gas Hydrates 6, 6-10 July, Paper 5636, Vancouver, 2008.

[5] Lee H, Yongwon S, Sea Y-T, Moudrakovski IL, Ripmeester JA. *Recovering methane from solid methane hydrate with carbon dioxide.* Angewandte Chemie 2003 DOI:10.1002/anie.200351489.

[6] Ota M, Morohashi K, Abe Y, Watanabe M, Smith RL Jr., Inomata H. *Replacement of* CH_4 *in the hydrate by use of liquid* CO_2. Energy Conversion and Management 2005;46 (11- 12): 1680-1691.

[7] Ota M, Saito T, Aida T, Watanabe M, Sato Y, Smith Jr RL, Inomata H. *Macro and microscopic* CH_4-CO_2 *replacement in* CH_4 *hydrate under pressurized* CO_2. AIChE J. 2007;53(10):2715- 2721.

[8] Park Y, Kim DY, Lee JW, Huh DG, Park KP, Lee J, Lee H. *Sequestering carbon dioxide into complex structures of naturally occurring gas hydrates*. PNAS. 2006;103(34):12690-12694.

[9] Stevens JC, Howard JJ, Baldwin BA, Ersland G, Husebø J, Graue A. E*xperimental hydrate formation and gas production scenarios based on* CO_2 *sequestration.* In: Proc. Intl. Conf. Gas Hydrates 6, 6-10 July, Paper 5635, Vancouver, 2008.

[10] Zhou XT, et al. *Replacement of methane from quartz-bearing hydrate with carbon dioxide-in- water emulsion*. Energy Fuels. 2008;22(3):1759- 1764.